ACS Partner Journal

Journal of the American Society for Mass Spectrometry

pubs.acs.org/jasms

Research Article

Structural Characterization of Natural and Synthetic Macrocycles Using Charge-Transfer Dissociation Mass Spectrometry

Halle M. Edwards, Zachary J. Sasiene, Praneeth M. Mendis, and Glen P. Jackson*

Cite This: *J. Am. Soc. Mass Spectrom.* 2022, 33, 671−680

Read Online

ACCESS | Metrics & More | Article Recommendations | Supporting Information

ABSTRACT: Research in natural products (NPs) has gained interest as drug developers turn to nature to combat problems with drug resistance, drug delivery, and emerging diseases. Whereas NPs offer a tantalizing source of new pharmacologically active compounds, their structural complexity presents a challenge for analytical characterization and organic synthesis. Of particular concern is the characterization of cyclic-, polycyclic-, or macrocyclic compounds. One example of endogenous compounds as inspiration for NP development are cobalamins, like vitamin B_{12}. An example of exogenous NPs is the class of macrolides that includes erythromycin. Both classes of macrocycles feature analogues with a range of modifications on their macrocyclic cores, but because of their cyclic nature, they are generally resistant to fragmentation by collision-induced dissociation (CID). In the present work, charge-transfer dissociation (CTD) was employed, with or without supplemental collisional activation, to produce radical-driven, high-energy fragmentation products of different macrocyclic precursors. With the assistance of collisional activation of CTnoD products, CTD frequently cleaved two covalent bonds within the macrocycle cores to reveal rich, informative spectra that helped identify sites of modification and resolve structural analogues. In a third example of macrocycle fragmentation, CTD enabled an impurity in a biological sample to be characterized as a cyclic polymer of nylon-6,6. In each example, CTD spectra are starkly different from CID and are highly reminiscent of other high-energy fragmentation techniques like extreme ultraviolet dissociative photoionization (XUV-DPI) and electron ionization-induced dissociation (EID). The results indicate that CTD-MS is a useful tool for the characterization of natural and synthetic macrocycles.

KEYWORDS: *ion activation, macrocyclic ions, macrolides, cobalamin, nylon-6,6, polymer*

INTRODUCTION

The need to create new therapeutics to treat infectious diseases has created a resurgence of research into natural products (NPs).[1] Prior to the development of modern synthetic drugs, people turned to plants and nature to remedy their ailments. Natural products are any compound produced from a living organism, but most pharmacologically active compounds tend to be metabolic products that plants and fungi use to protect themselves from predation.[2,3] Some famous examples of drugs derived from NPs include aspirin, which has its origins in willow tree bark,[4] and opioids like morphine, which are derived from the poppy plant.[5] Even as drug development grew out of the textile and dye industries in the second half of the 20th century, most synthetic drugs were derived from, or inspired by, a natural compound.[6,7]

Many NPs have complex structures—including cyclic-, polycyclic-, or macrocyclic rings—which can make them difficult to both characterize and synthesize. One example of the potential structural complexity can be found with vitamin B_{12} (Figure 1), a critical coenzyme for many bodily functions in animals. The structure of vitamin B_{12} was outlined in 1956[8] but was not fully synthesized until nearly 20 years later by Woodward's group.[9] Vitamin B_{12} has been demonstrated to be a promising drug delivery tool when certain active sites on the molecule are modified, so the ability to obtain comprehensive MS/MS characterization of vitamin B_{12} could facilitate it is development as a novel drug or drug-delivery tool.[10] The structural characterization of compounds like vitamin B_{12} is also important in cancer research, where rapidly growing cancer cells have an increased demand for essential vitamins like vitamin B_{12}. Delivering modified versions of vitamin B_{12} can target and disrupt the replication of cancer cells,[11] and the exaggerated uptake of vitamin B_{12} by cancer cells can be useful in imaging applications that dose patients with fluorophore-modified versions of vitamin B_{12}.[12]

Received: December 16, 2021
Revised: February 9, 2022
Accepted: February 10, 2022
Published: February 23, 2022

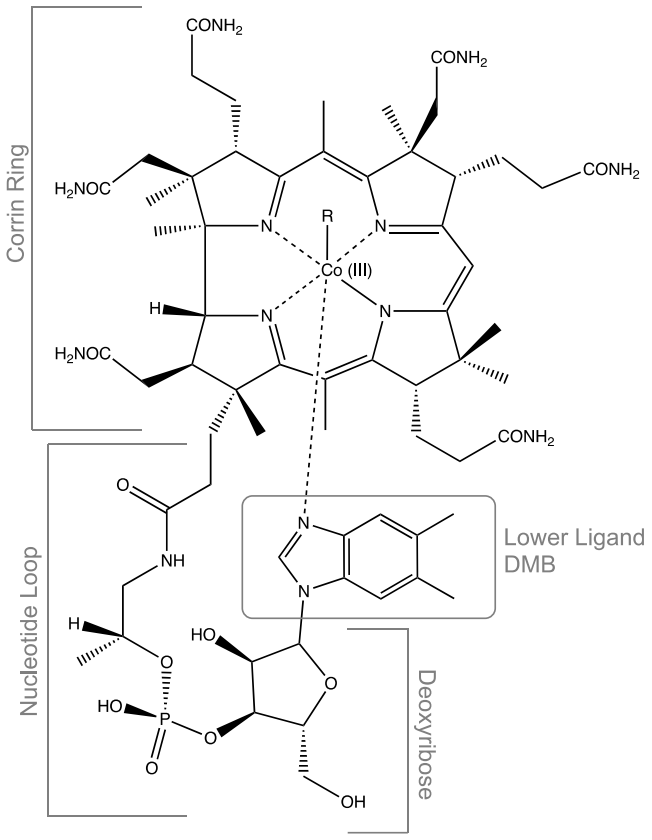

Figure 1. Basic structure of vitamin B_{12} or cobalamin. R represents one of three substituents for the most common forms of vitamin B_{12}: −OH for hydroxocobalamin, −CN for cyanocobalamin, and $-CH_3$ for methylcobalamin. Major structural components indicated. DMB represents 5,6-dimethylbenzimidazole.

Vitamin B_{12} contains a polycyclic porphyrin ring, a cyclic sugar, a cyclic benzimidazole region, and a macrocyclic structure when the benzimidazole ligand bonds to cobalt in the core of the porphyrin ring (Figure 1). These ring structures tend to limit the extent of structural information obtained by collision-induced dissociation (CID), especially because of the presence of labile bonds and leaving groups, like the phosphate group and the monodentate cobalt ligand.[13−17]

Polycyclic and macrocyclic NPs are very common in nature. Erythromycin is a widely used antibiotic that is derived from the soil bacteria *Saccharopolyspora erythraea.* Erythromycin contains a characteristic macrocyclic ring known as a macrolide.[18,19] Since its development in 1952, erythromycin has been modified in a variety of ways to create several NPs with different uses and activities.[20,21,30,31,22−29] These variants are commonly referred to as erythromycins A−D. When erythromycin is characterized using commonly available mass spectrometric techniques like CID, the tandem mass spectra are dominated by successive water losses that provide very little structural information.[32,33] Other higher-energy techniques, like EID[34] and XUV-DPI,[35] provide more extensive fragmentation of erythromycins, richer spectra, and significantly more structural information than CID.

Cyclic synthetic polymers have been investigated as important drug delivery tools because they often have a greater drug loading capacity than other molecules and they can help deliver drugs that have poor solubility on their own.[36,37] Drugs paired with cyclic polymers can offer a longer circulation time in the blood and provide a more controlled release with longer efficacy.[36,37] However, the fragmentation of cyclic polymers results in successive losses of monomers, which reveals little about the structure of the monomers.[38,39]

The ability to observe fragment ions from macrocycles relies on the ability to cleave multiple covalent bonds following each activation. Toward this end, CTD has demonstrated the ability to break two covalent bonds in single activation events in several cases: (1) to form cross-ring fragments of hexose rings in oligosaccharides,[40−47] (2) to form backbone cleavages of proteins within disulfide-linked proteins,[48] and (3) to form *d* and *w* ions of peptides.[49,50] CTD uses kiloelectronvolt helium cations in the range of 3−10 keV for ion activation. Helium is used because it has the highest electron affinity of any singly charged cation at 24.6 eV, although there is significant evidence that the kinetic energy of the reagent ion is responsible for most of the available excitation energy during activation, so CTD efficiencies are not sensitive to the ionization potential of the reagent ion.[51,52] CTD initially produces doubly charged radical cations (from singly charged precursors) that usually dissociate rapidly through radical-driven fragmentation pathways. When the oxidized product ion does not fragment, the observed peak is termed the charge transfer no dissociation (CTnoD) peak, consistent with the naming system of other electron-based activation methods.

In this paper, we investigate the ability of CTD to provide fragmentation of three different types of challenging macrocycles. First, we studied vitamin B_{12}, which features a central corrin ring along with two axial ligands coordinated to a central cobalt ion.[8,53] Second, we investigated the fragmentation of different macrolide antibiotics: erythromycins A−C. Finally, we investigated the fragmentation behavior of an interferent in the analysis of a glycan experiment, which was identified as a cyclic polymer of nylon-6,6. Whereas nylon is not an NP, it is a common contaminant in MS/MS and LC−MS experiments, and its amide linkages bear structural similarity to many natural prodcuts.[54,55] Detailed characterization of these important classes of macrocycles can have far reaching impacts in drug discovery, development, and delivery. The results indicate that CTD on a benchtop ion trap mass spectrometer produces significantly more structurally informative fragments than can be accomplished using conventional tandem mass spectrometry approaches such as CID.

METHODS

Instrumentation. CTD and CID experiments were performed on a modified Bruker amaZon 3D ion trap mass spectrometer (Bruker Daltonics, Bremen, Germany). To perform CTD, a saddle field fast ion source interfaced with the vacuum cover lid was mounted directly above a 3 mm hole in the ring electrode of the ion trap. A pulsed high voltage to the anode of the ion gun is timed to permit ∼6 keV helium ions into the trap for periods ranging from 20 to 100 ms. Full instrument modifications are described elsewhere.[49,50,56] UHP helium from Matheson TRIGAS (Fairmont, WV) was used as the reagent gas for all experiments, although recent work has shown that the nature and purity of the reagent gas might not be important.[52]

Samples. Vitamin B_{12} (cyanocobalamin and methylcobalamin) was purchased from Sigma-Aldrich (St. Louis, MO). Erythromycin A was purchased from Acros Organics (Palo Alto, CA), and erythromycins B and C are European Pharmacopoeia reference standards from the European Directorate for the Quality of Medicines (Strasbourg, France). All solutions were prepared in a water/methanol/formic acid mixture (49.5:49.5:1

https://doi.org/10.1021/jasms.1c00369
J. Am. Soc. Mass Spectrom. 2022, 33, 671−680

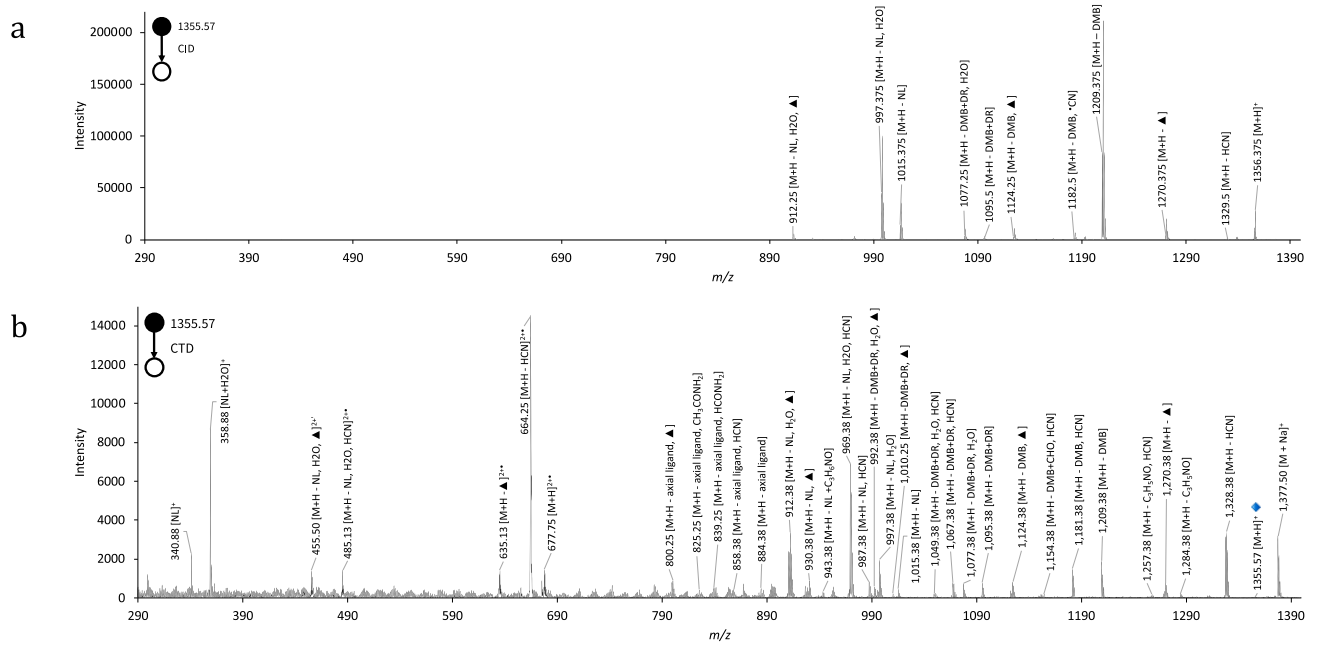

Figure 2. (a) CID spectrum of cyanocobalamin and (b) CTD spectrum of cyanocobalamin. ▲ represents a loss of either CoCN (84.94 Da) or •CN and CH_3CONH_2 (85.04 Da). Abbreviations are as follows: DMB = 5,6-dimethylbenzimidazole base ($C_9H_{10}N_2$, 146.08 Da); DMB+DR = 5,6-dimethylbenzimidazole base and deoxy ribose sugar ($C_{14}H_{16}O_3N_2$, 261.12 Da); NL = nucleotide loop ($C_{14}H_{17}N_2O_6P$, 340.08 Da).

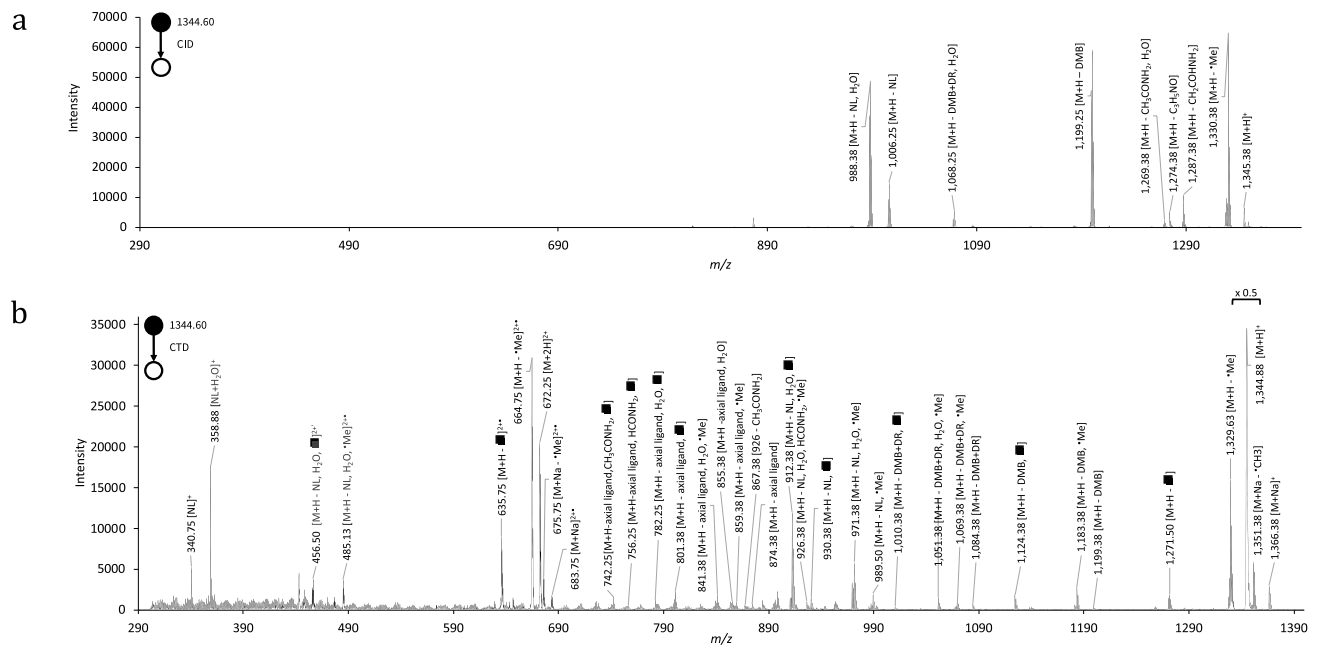

Figure 3. (a) CID spectrum of methylcobalamin, and b) CTD spectrum of methylcobalamin. ■ represents a loss of either $CoCH_3$ (73.96 Da) or •CH_3 and CH_3CONH_2 (74.06 Da). Abbreviations are as follows: DMB = 5,6-dimethylbenzimidazole base ($C_9H_{10}N_2$, 146.08 Da); DMB+DR = 5,6-dimethylbenzimidazole base and deoxy ribose sugar ($C_{14}H_{16}O_3N_2$, 261.12 Da); NL = nucleotide loop ($C_{14}H_{17}N_2O_6P$, 340.08 Da).

v/v/v) with a final concentration of 100 ppm. HPLC-grade methanol and formic acid (Fisher Scientific, Fair Lawn, NJ) were used for sample preparation.

Method. Vitamin B_{12} solutions were introduced to the MS inlet with an electronic syringe pump at a flow rate of 5.0 μL/min and a voltage of 3.5 kV. Erythromycin samples were ionized by a static nanospray source at a voltage of 1500 V. The low mass cutoff (LMCO) was set to m/z 250, and an isolation width of 4 Da was used for all experiments. CID experiments were performed with a reaction amplitude of 0.5−1.5 V. For CTD experiments, fragmentation was achieved by exposing precursor ions to 5−7 keV helium cations pulsed for 100 ms. A leak valve maintained the flow of helium into the vacuum chamber at 1.2×10^{-5} mbar. To prevent unwanted space charge effects, any unreacted precursor ions remaining after CTD were resonantly ejected with a CID amplitude of 1.0−7.0 V before mass acquisition.

https://doi.org/10.1021/jasms.1c00369
J. Am. Soc. Mass Spectrom. 2022, 33, 671−680

For experiments with nylon-6,6, the singly charged precursor at m/z 453.3 was isolated and then fragmented by CTD. The doubly charged product ion at m/z 226.5 was then isolated and fragmented by CID at the MS^3 level. The LMCO was set to m/z 50, and the CID amplitude was 0.8 V.

RESULTS AND DISCUSSION

Vitamin B_{12}. Tables of fragments of CID and CTD of cyanocobalamin and methylcobalamin are provided in Tables S1−S4. CID of vitamin B_{12} produced relatively few product ions and is restricted to fragments above m/z 900 (Figure 2a). Most of the product ions in the CID spectra arise from neutral losses of the major structural components, including the 5,6-dimethylbenzimidazole base (DMB, $C_9H_{10}N_2$, 146.08 Da), the combined loss of 5,6-dimethylbenzimidazole base and deoxy ribose sugar (DMB+DR, $C_{14}H_{16}O_3N_2$, 261.12 Da), and the nucleotide loop (NL, $C_{14}H_{17}N_2O_6P$, 340.08 Da). Peaks corresponding to one or more neutral water losses from these fragments are also observed (Figures 2a and 3a).

When comparing CID and CTD of protonated vitamin B_{12}, CTD produces many more fragments across a wider range of m/z values. Most of the product ions from CTD derive from cleavages within the nucleotide loop. CID also forms a few products in this region, but not to the same extent. In addition to cleavages within the nucleotide loop, CTD and CID also induce the losses of water and other small molecules from many of the product ions. For example, with cyanocobalamin (CNCbl), CTD produces several product ions that include neutral losses of HCN, which must involve a rearrangement of hydrogen atom to the cyanide group bonded to the central cobalt ion (Figure 4). In contrast, CID of cyanocobalamin does not produce any analogous losses of HCN. Likewise, with methylcobalamin (MeCbl), which has a methyl group coordinated to the central cobalt, the CTD spectrum contains many instances of a methyl radical loss, but the CID spectrum does not (Figure 3). The fragment ion map of methylcobalamin is provided in Figure S1.

Unique to the CTD spectra of CNCbl and MeCbl are losses of 85 and 74 Da. These losses are most likely the loss of the central cobalt along with the axial ligand (−CoCN, 84.94 Da; $-CoCH_3$, 73.96 Da). However, the limited mass resolution of our instrument prevents confident assignment of these neutral losses because the peaks are nominally isobaric with the loss of the axial ligand plus one of the acetamide groups along the perimeter of the corrin ring ($^{\bullet}CN$ and CH_3CONH_2 = 85.04 Da; $^{\bullet}CH_3$ and CH_3CONH_2 = 74.06 Da). The extensive fragmentation along the various parts of the macrocyclic region suggests that any additional modifications along the macrocycle would be more readily identified using CTD than CID. The richness of the CTD spectra are consistent with the ability to break two or more covalent bonds in a single activation event, and with the ability to provide access to higher energy, radical-driven pathways that cause fragmentation away from the charge site and the most labile bonds.

Erythromycins. Erythromycins A, B, and C (EA, EB, and EC) differ in the presence of hydroxy or methoxy substitutions at two different locations on the macrocycle. One site of substitution is on the C3 position of the cladinose ring, and the other is in the C12 position of the macrocyclic ring. Collision-induced dissociation of EA, EB, and EC results in spectra (Figure S2) that are dominated by the loss(es) of the cladinose and/or mycarose groups from the macrocycle and successive water losses thereof. The spectra contain little structural information about the macrolide itself. The neutral loss

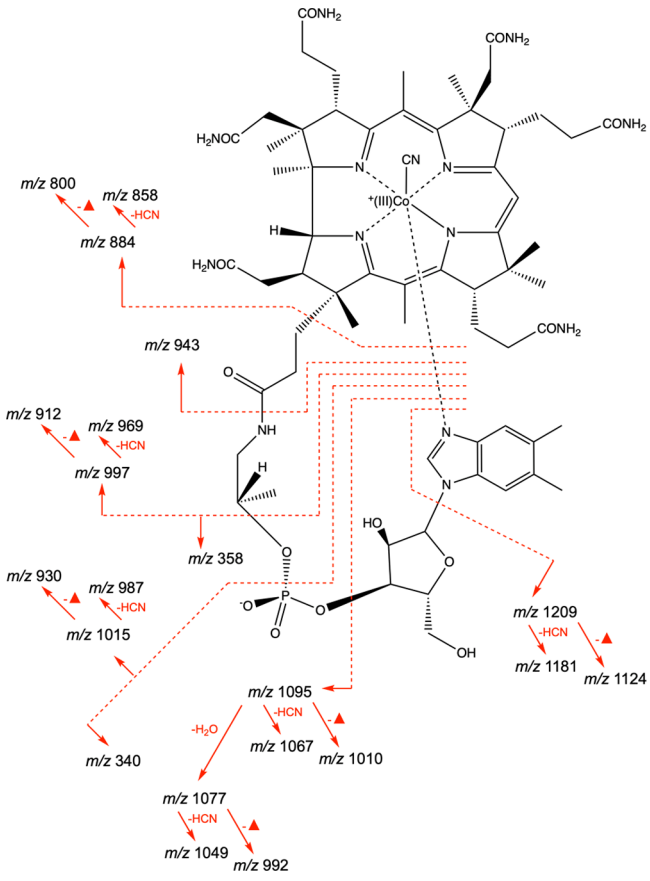

Figure 4. CTD fragmentation diagram of cyanocobalamin. ▲ represents a loss of either CoCN (84.94 Da) or $^{\bullet}CN$ and CH_3CONH_2 (85.04 Da).

differences between the three structures indicate differences in the sugars attached to the macrocycle, but nothing can be inferred about the structure of the sugars or their location in the macrolide. In these respects, the CID results obtained here are qualitatively consistent with previous CID studies.[32,33,57,58]

CTD of erythromycins A−C provided a greater number and greater diversity of fragments than CID (Figure 5a−c). For each sample, CTD provided extensive fragmentation of the macrocyclic ring, and some fragments were accompanied by a cross-ring cleavage of one of the sugar groups. The fragmentation patterns and the identified peaks are very similar to those produced in the previous work of others using EID or XUV-DPI with high mass accuracy detection.[34,35] The fragments are outlined in Table 1, and the fragmentation nomenclature follows that outlined by Wills.[34] All three dissociation methods (EID, XUV-DPI, and CTD) produce the same cross-ring cleavage (BD) of the cladinose ring. This same cross-ring cleavage is produced with CTD of precursors of erythromycins B and C, which makes the ion an important fragment for pinpointing the modification position within the attached sugar. CTD also produces a cross ring cleavage of the desosamine sugar for erythromycins A and B. Specific cleavages of the macrocyclic ring—including fragments IL, FG, and NP-H_2O—are also observed with XUV-DPI, EID, and CTD. Many of the neutral losses reported with EID are observed in the CTD spectra, particularly the neutral losses following loss of the cladinose sugar (fragment E).

Macrolide analogues contain a variety of chemical modifications within the sugar groups and along the macrocycle, and

https://doi.org/10.1021/jasms.1c00369
J. Am. Soc. Mass Spectrom. 2022, 33, 671−680

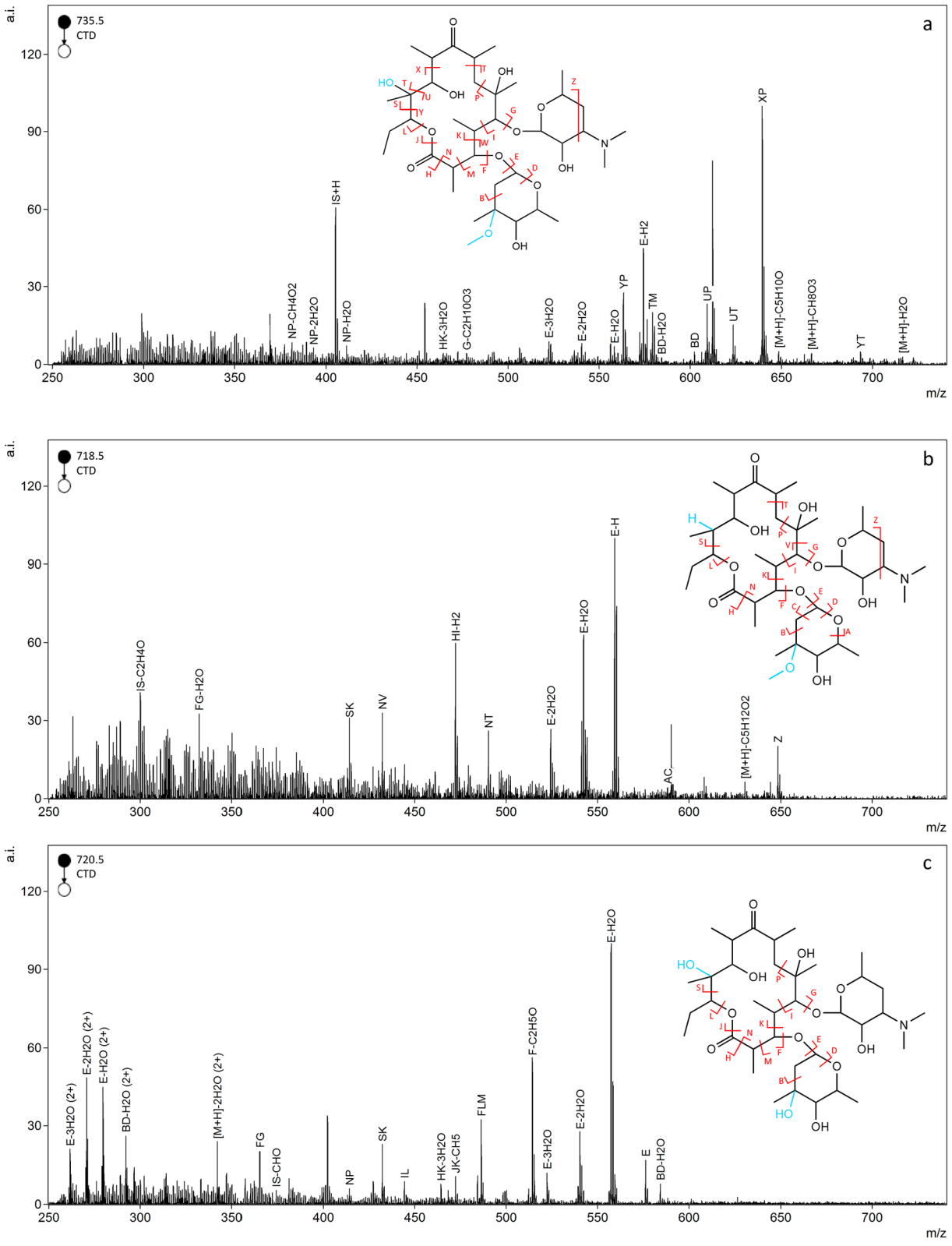

Figure 5. CTD spectra of (a) erythromycin A, (b) erythromycin B, and (c) erythromycin C with inset fragment maps.

the ability to pinpoint and identify these modifications is critical to distinguishing isomers and metabolites. Intrasugar cross-ring cleavages can provide information about modification positions within the sugar groups, whereas multiple cleavages along the macrocycle can pinpoint and identify changes in the macrolide ring. Erythromycins A and C only differ in the nature of the cladinose sugar, so any cleavages that involve the elimination of the cladinose sugar should fall at the same mass. As an example, a neutral loss of the cladinose sugar group (−158 Da for EA and −144 Da for EC) results in a peak at m/z 576.4 for both EA and EC, which localizes any modifications to the lost sugar group rather than within the macrocycle. Erythromycin B differs from

https://doi.org/10.1021/jasms.1c00369
J. Am. Soc. Mass Spectrom. 2022, 33, 671−680

Table 1. Summary of fragments of Erythromycin A Using Three Different Dissociation Methods

m/z	XUV-DPI[35]	EID[34]	CTD
716.5	$[M + H - H_2O]^+$	$[M + H - H_2O]^+$	$[M + H - H_2O]^+$
648.4	$[M + H - C_5H_{10}O]^+$	$[M + H - C_5H_{10}O]^+$	$[M + H - C_5H_{10}O]^+$
630.4	$[M + H - C_5H_{12}O_2]$	$[M + H - C_5H_{12}O_2]^+$	
602.4	BD	BD	BD
584.4		BD − H_2O	BD − H_2O
576.4	E	E	E
575.4	E-H	E − H	E − H
574.4		E − H_2	E − H_2
560.3		E − CH_4	E − CH_4
558.4		E − H_2O	E − H_2O
557.4		E − H_2O -H	E − H_2O -H
556.3		E − H_2O − H_2	E − H_2O − H_2
542.4		E − H_2O_2	E − H_2O_2
540.4	E − $2H_2O$	E − $2H_2O$	E − $2H_2O$
522.3	E − $3H_2O$	E − $3H_2O$	E − $3H_2O$
514.3	F − C_2H_5O	F − C_2H_5O	
490.3	HI	HI	
489.3		JK	JK
477.3		G − $C_2H_{10}O_3$	G − $C_2H_{10}O_3$
472.3	JK-CH_5	JK − CH_5	JK − CH_5
464.3		HK − $3H_2O$	HK − $3H_2O$
444.3	IL	IL	IL
429.2		NP	NP
411.2	NP − H_2O	NP − H_2O	NP − H_2O
393.2	NP − $2H_2O$	NP − $2H_2O$	NP − $2H_2O$
381.2	NP − CH_4O_2	NP − CH_4O_2	NP − CH_4O_2
365.2	FG	FG	FG

EA only in a single substituent on the macrocycle. The loss of the cladinose sugar (−158 Da) from EB results in a peak at *m/z* 559.4, indicative of the structural differences between EA and EB along the macrocyclic ring. Furthermore, several identified peaks in the EB spectrum are observed to be 16 Da less than the same peaks within the EA spectra, which helps identify the modification as an oxygen.

Nylon. While conducting CTD experiments of a laminarin sample[45] we noted a consistent singly charged peak was observed at *m/z* 453.3 in full mass scanning. The peak was accompanied by an $[M + Na]^+$ peak at *m/z* 475.3 and an $[M + K]^+$ peak at *m/z* 491.3, and all three peaks were determined to derive from the use of a nylon membrane filter during sample preparation. To confirm the identity of the substance, we subjected the protonated precursor at *m/z* 453.3 to CID and CTD. Upon CTD fragmentation of the $[M + H]^+$ precursor, very few fragments were produced other than an intense $[M + H]^{2+}$* ion at *m/z* 226.6. However, CID of the CTnoD product ion at *m/z* 226.6, at the MS^3 level, produced several product ions in the region *m/z* 70−453. Previous work has shown that CID fragmentation of radicals generated from CTD or metastable atom activated dissociation (MAD) can be a useful approach to obtaining richer spectra with superior S/N than CTD or MAD alone.[48,56] Based on the fragmentation pattern, the unknown peak was found to be a cyclic polymer of Nylon-6,6, which is a reported contaminant commonly found in MS/MS and LC−MS experiments.[54,55]

The intense CTnoD peak, $[M + H]^{2+}$*, is caused by the cleavage of one covalent bond in the macrocycle, which does not produce any neutral losses because the "fragments" are still covalently bound through the macrocycle structure (Scheme 1). However, additional activation through CID at the MS^3 level activates the radical species and results in the information-rich spectrum in Figure 6b.

One challenge in identifying the unknown contaminant was in determining if it was a cyclic tetramer of Nylon-6 or a cyclic dimer of Nylon-6,6 because the two species are isobaric and both have been identified as common contaminants in MS/MS experiments. A Nylon-6 monomer contains 6 carbons and the repeat unit weighs 113.16 g/mol.[59] If the unknown species were a Nylon-6 tetramer, then one would expect to see multiple losses of 113 Da in the CID spectra, which would correspond to successive monomer losses. As shown in Figure 6a, no such losses are observed, so Nylon-6 can be excluded. Nylon-6,6 has a repeat unit of 226.32 g/mol[60] and a CID peak corresponding to the loss of a Nylon-6,6 monomer is observed as a singly charged product at *m/z* 226.2. Comparison to previously reported MS/MS spectra of Nylon-6,6 confirmed the identity of this unknown contaminant to be a cyclic dimer of Nylon-6,6.[54]

The fragments produced from CID of the precursor at *m/z* 453.3 and CID of the CTnoD product ion at *m/z* 226.6 are shown in Figure 6. The CID fragments are labeled according to those outlined by Tran and Doucette.[54] CTD-CID product ions are distributed throughout the polymer chain and provide much greater coverage of the molecule. Had mixed monomers been present, the extensive fragmentation in the CTD-CID spectrum presumably could have provided clarification into mixed monomer units and could have helped pinpoint any modifications along the polymer chain.

The combination of CTD-CID could be a useful tool for characterizing other difficult-to-fragment cyclic polymers. Not only does CTD initiate ring opening, but CTD-CID also generates a radical species that generally produces more abundant and informative product ions than can be obtained

Scheme 1. Proposed Pathway for the formation of the CTnoD Product Ion at *m/z* 226.6

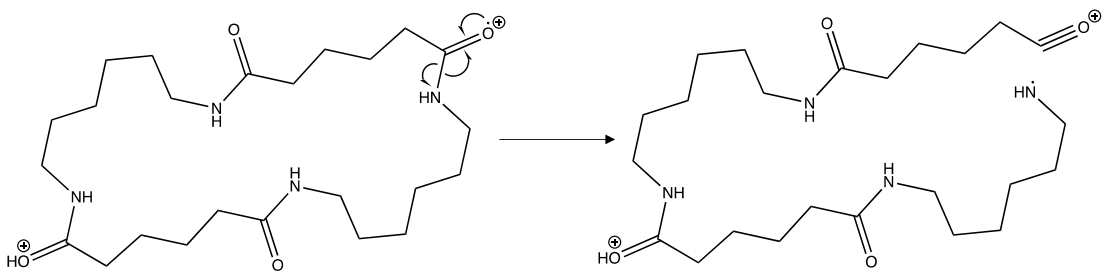

https://doi.org/10.1021/jasms.1c00369
J. Am. Soc. Mass Spectrom. 2022, 33, 671−680

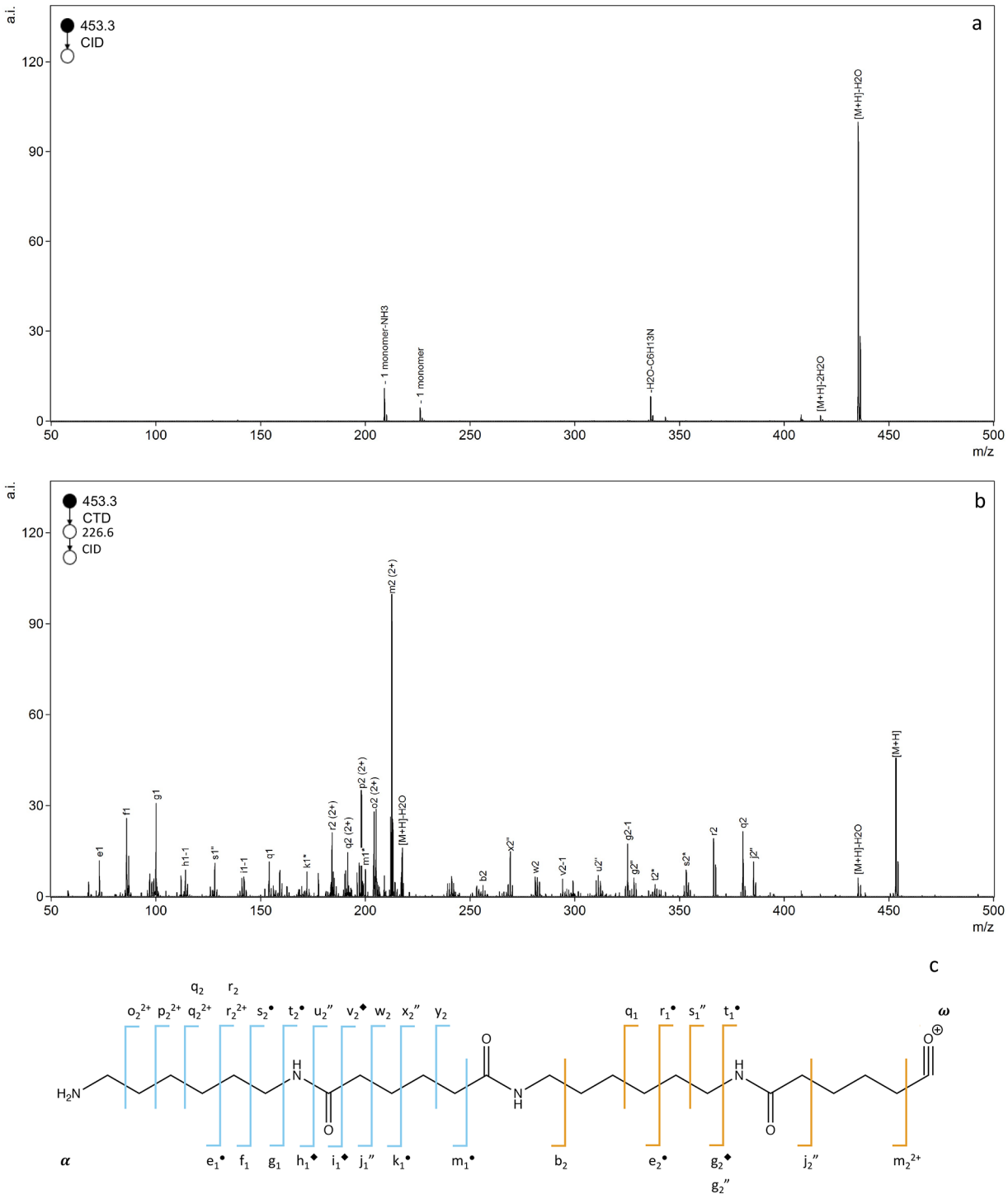

Figure 6. (a) CID fragmentation of $[M + H]^+$ peak at m/z 453.3 and (b) CTD-CID fragmentation of Nylon-6,6 at m/z 226.6. (c) Nomenclature follows that outlined by Polce[61] with the addition of the ♦ superscript to designate −2H observed with CTD. Fragments in blue correspond to the first monomer unit, while fragments in orange correspond to the second monomer unit.

with traditional CID. In comparison to other high energy techniques, CTD-CID may outperform ECD of synthetic polymers, which has been reported to provide limited information beyond that obtained by CID.[62]

CONCLUSIONS

CTD produces a greater distribution of fragment ions from macrocyclic structures than conventional fragmentation approaches like CID. In cases where comparisons to EID and XUV-DPI are possible, CTD spectra show considerable similarities with the other high energy and radical fragmentation approaches, with the benefit that CTD can be performed on an instrument as simple as a benchtop ion trap. The enhanced fragmentation afforded by CTD allows for more confident structural determinations, which can be vital to the biological functions and modifications in biochemical systems. In addition, we have demonstrated CTD as a new method to generate radical species from cyclic polymers, which allows for simpler and more

https://doi.org/10.1021/jasms.1c00369
J. Am. Soc. Mass Spectrom. 2022, 33, 671−680

informative sequencing when subjected to CID at the MS^3 level of fragmentation. Whereas CTD provides rich and informative spectra, the mass resolution of the current instrument limits some spectral interpretations because of the isobaric nature of some of the product ions. The ability to perform CTD with high resolution mass spectrometry would be helpful in elucidating some neutral losses and providing greater confidence in the identity of the fragment ions.

■ ASSOCIATED CONTENT

Supporting Information

The Supporting Information is available free of charge at https://pubs.acs.org/doi/10.1021/jasms.1c00369.

CTD fragment map for methylcobalamin (MeCbl); peak lists for CID and CTD of CNCbl and MeCb; CID spectra for erythromycins A−C (PDF)

■ AUTHOR INFORMATION

Corresponding Author

Glen P. Jackson − *Department of Forensic and Investigative Science and C. Eugene Bennett Department of Chemistry, West Virginia University, Morgantown, West Virginia 26506, United States;* orcid.org/0000-0003-0803-6254; Phone: 304-293-9236; Email: glen.jackson@mail.wvu.edu

Authors

Halle M. Edwards − *C. Eugene Bennett Department of Chemistry, West Virginia University, Morgantown, West Virginia 26506, United States*

Zachary J. Sasiene − *C. Eugene Bennett Department of Chemistry, West Virginia University, Morgantown, West Virginia 26506, United States;* Present Address: Bioscience Division, Los Alamos National Laboratory, Los Alamos, NM 87545

Praneeth M. Mendis − *C. Eugene Bennett Department of Chemistry, West Virginia University, Morgantown, West Virginia 26506, United States*

Complete contact information is available at: https://pubs.acs.org/10.1021/jasms.1c00369

Notes

The authors declare no competing financial interest.

■ ACKNOWLEDGMENTS

We acknowledge financial support from the National Science Foundation (NSF) (CHE-1710376) and the National Institute of Health (NIH) (1R01GM114494-01). The opinions, findings, and conclusions or recommendations expressed in this publication are those of the authors and do not necessarily reflect the views of the NSF or NIH.

■ REFERENCES

(1) *Natural Products Analysis: Instrumentation, Methods, and Applications*, 1st ed.; Havlicek, V., Spizek, J., Eds.; John Wiley & Sons: Hoboken, NJ, 2014.

(2) Maplestone, R. A.; Stone, M. J.; Williams, D. H. The Evolutionary Role of Secondary Metabolites - a Review. *Gene* **1992**, *115* (1−2), 151−157.

(3) Li, J. W. H.; Vederas, J. C. Drug Discovery and Natural Products: End of an Era or an Endless Frontier? *Science (80-.).* **2009**, *325* (5937), 161−165.

(4) Schrör, K. *Acetylsalicylic Acid*; Wiley-VCH: Weinheim, Germany, 2010.

(5) Busse, G. D. *Morphine*; Triggle, D. J., Ed.; Chelsea House: New York, NY, 2006.

(6) Sneader, W. *Drug Prototypes and Their Exploitation*, 1st ed.; John Wiley & Sons: Hoboken, NJ, 1996.

(7) Jones, A. W. Early Drug Discovery and the Rise of Pharmaceutical Chemistry. *Drug Test. Anal.* **2011**, *3* (6), 337−344.

(8) Hodgkin, D. C.; Kamper, J.; MacKay, M.; Pickworth, J.; Trueblood, K. N.; White, J. G. Structure of Vitamin B12. *Nature* **1956**, *178* (4524), 64−66.

(9) Woodward, R. B. The Total Synthesis of Vitamin B12. *Pure Appl. Chem.* **1973**, *33* (1), 145−178.

(10) Clardy, S. M.; Allis, D. G.; Fairchild, T. J.; Doyle, R. P. Vitamin B 12 in Drug Delivery: Breaking through the Barriers to a B 12 Bioconjugate Pharmaceutical. *Expert Opin. Drug Delivery* **2011**, *8* (1), 127−140.

(11) Waibel, R.; Treichler, H.; Schaefer, N. G.; Van Staveren, D. R.; Mundwiler, S.; Kunze, S.; Küenzi, M.; Alberto, R.; Nüesch, J.; Knuth, A.; Moch, H.; Schibli, R.; Schubiger, P. A. New Derivatives of Vitamin B12 Show Preferential Targeting of Tumors. *Cancer Res.* **2008**, *68* (8), 2904−2911.

(12) Smeltzer, C. C.; Cannon, M. J.; Pinson, P. R.; Munger, J. D., Jr; West, F. G.; Grissom, C. B. Synthesis and Characterization of Fluorescent Cobalamin (CobalaFluor) Derivatives for Imaging. *Org. Lett.* **1997**, *3* (6), 799−801.

(13) He, L.; Wei, G.; Murray, K. K. Fragmentation of Vitamin B12 in Aerosol Matrix-Assisted Laser Desorption Ionization. *J. Am. Soc. Mass Spectrom.* **1997**, *8*, 140−147.

(14) Bito, T.; Bito, M.; Asai, Y.; Takenaka, S.; Yabuta, Y.; Tago, K.; Ohnishi, M.; Mizoguchi, T.; Watanabe, F. Characterization and Quantitation of Vitamin B 12 Compounds in Various Chlorella Supplements. *J. Agric. Food Chem.* **2016**, *64*, 8516−8524.

(15) Barber, M.; Bordoli, R. S.; Sedgwick, R. D.; Tyler, A. N. Fast Atom Bombardment Mass Spectrometry of Cobalamines. *Biomed. Mass Spectrom.* **1981**, *8* (10), 492−495.

(16) Luo, X.; Chen, B.; Ding, L.; Tang, F.; Yao, S. HPLC-ESI-MS Analysis of Vitamin B 12 in Food Products and in Multivitamins-Multimineral Tablets. *Anal. Chim. Acta* **2006**, *562*, 185−189.

(17) Calvano, C. D.; Ventura, G.; Palmisano, F.; Cataldi, T. R. I. 4-Chloro-α-Cyanocinnamic Acid Is an Efficient Soft Matrix for Cyanocobalamin Detection in Foodstuffs by Matrix-Assisted Laser Desorption/Ionization Mass Spectrometry (MALDI MS). *J. Mass Spectrom.* **2016**, *51*, 841−848.

(18) Wiley, P. F.; Gerzon, K.; Flynn, E. H.; Sigal, M. V.; Weaver, O.; Quarck, U. C.; Chauvette, R. R.; Monahan, R. Erythromycin. X. Structure of Erythromycin. *J. Am. Chem. Soc.* **1957**, *79* (22), 6062−6070.

(19) *Biosynthesis: Polyketides and Vitamins*; Leeper, F. J., Vederas, J. C., Eds.; Springer-Verlag: Berlin Heidelberg, Germany, 2000.

(20) Kibwage, I. O.; Hoogmartens, J.; Roets, E.; Vanderhaeghe, H.; Verbist, L.; Dubost, M.; Pascal, C.; Petitjean, P.; Levol, G. Antibacterial Activities of Erythromycins A, B, C, and D and Some of Their Derivatives. *Antimicrob. Agents Chemother.* **1985**, *28* (5), 630−633.

(21) Hogan, P. C.; Chen, C.-L.; Mulvihill, K. M.; Lawrence, J. F.; Moorhead, E.; Rickmeier, J.; Myers, A. G. Large-Scale Preparation of Key Building Blocks for the Manufacture of Fully Synthetic Macrolide Antibiotics. *J. Antibiot. (Tokyo).* **2018**, *71*, 318−325.

(22) Seiple, I. B.; Zhang, Z.; Jakubec, P.; Langlois-Mercier, A.; Wright, P. M.; Hog, D. T.; Yabu, K.; Rao Allu, S.; Fukuzaki, T.; Carlsen, P. N.; Kitamura, Y.; Zhou, X.; Condakes, M. L.; Szczypiński, F. T.; Green, W. D.; Myers, A. G. A Platform for the Discovery of New Macrolide Antibiotics. *Nature* **2016**, *533*, 338−345.

(23) Morimoto, S.; Takahashi, Y.; Watanabe, Y.; Omura, S. Chemical Modification of Erythromycins. I. Synthesis and Antibacterial Activity of 6-O-Methylerythromycins A. *J. Antibiot. (Tokyo).* **1984**, *37*, 187−189.

(24) Martin, S. F.; Hida, T.; Kym, P. R.; Loft, M.; Hodgson, A. The Asymmetric Synthesis of Erythromycin B. *J. Am. Chem. Soc.* **1997**, *119*, 3193−3194.

(25) Cyphert, E.; Wallat, J.; Pokorski, J.; von Recum, H. Erythromycin Modification That Improves Its Acidic Stability While Optimizing It for Local Drug Delivery. *Antibiotics* **2017**, *6* (2), 11.
(26) Kim, H. C.; Kang, S. H. Total Synthesis of Azithromycin. *Angew. Chemie Int. Ed.* **2009**, *48* (10), 1827−1829.
(27) Andrade, R. Total Synthesis of Desmethyl Macrolide Antibiotics. *Synlett* **2015**, *26* (16), 2199−2215.
(28) Somberg, J.; Ranade, V. Synthesis and Separation of Optically Active Isomers of Erythromycin and Their Biological Actions. US 2004/0067898 A1, 2004.
(29) Putnam, S. D.; Castanheira, M.; Moet, G. J.; Farrell, D. J.; Jones, R. N. CEM-101, a Novel Fluoroketolide: Antimicrobial Activity against a Diverse Collection of Gram-Positive and Gram-Negative Bacteria. *Diagn. Microbiol. Infect. Dis.* **2010**, *66*, 393−401.
(30) Cevallos, A.; Guerriero, A. Isolation and Structure of a New Macrolide Antibiotic, Erythromycin G, and a Related Biosynthetic Intermediate from a Culture of Saccharopolyspora Erythraea. *J. Antibiot. (Tokyo).* **2003**, *56* (3), 280−288.
(31) Woodward, R. B.; Logusch, E.; Nambiar, K. P.; Sakan, K.; Ward, D. E.; Au-Yeung, B. W.; Balaram, P.; Browne, L. J.; Card, P. J.; Chen, C. H.; Chenevert, R. B.; Fliri, A.; Frobel, K.; Gals, H. J.; Garratt, D. G.; Hayakawa, K.; Heggie, W.; Hesson, D. P.; Hoppe, D.; Hoppe, I.; Hyatt, J. A.; Ikeda, D.; Jacobi, P. A.; Kim, K. S.; Kobuke, Y.; Kojima, K.; Krowicki, K.; Lee, V. J.; Leutert, T.; Malchenko, S.; Martens, J.; Matthews, R. S.; Ong, B. S.; Press, J. B.; Rajan Babu, T. V.; Rousseau, G.; Sauter, M.; Suzuki, M.; Tatsuta, K.; Tolbert, L. M.; Truesdale, E. A.; Uchida, I.; Ueda, Y.; Uyehara, T.; Vasella, A. T.; Vladuchick, W. C.; Wade, P. A.; Williams, R. M.; Wong, H. N.-C. Asymmetric Total Synthesis of Erythromycin. 3. Total Synthesis of Erythromycin. *J. Am. Chem. Soc.* **1981**, *103*, 3215−3217.
(32) Gates, P. J.; Kearney, G. C.; Jones, R.; Leadlay, P. F.; Staunton, J. Structural Elucidation Studies of Erythromycins by Electrospray Tandem Mass Spectrometry. *Rapid Commun. Mass Spectrom.* **1999**, *13*, 242−246.
(33) Kearney, G. C.; Gates, P. J.; Leadlay, P. F.; Staunton, J.; Jones, R. Structural Elucidation Studies of Erythromycins by Electrospray Tandem Mass Spectrometry II. *Rapid Commun. Mass Spectrom.* **1999**, *13*, 1650−1656.
(34) Wills, R. H.; Tosin, M.; O'connor, P. B. Structural Characterization of Polyketides Using High Mass Accuracy Tandem Mass Spectrometry. *Anal. Chem.* **2012**, *84*, 8863−8870.
(35) Giuliani, A.; Williams, J. P.; Green, M. R. Extreme Ultraviolet Radiation: A Means of Ion Activation for Tandem Mass Spectrometry. *Anal. Chem.* **2018**, *90*, 7176−7180.
(36) Golba, B.; Benetti, E. M.; De Geest, B. G. Biomaterials Applications of Cyclic Polymers. *Biomaterials*; Elsevier, Ltd., 2021; p 120468. DOI: DOI: 10.1016/j.biomaterials.2020.120468.
(37) Liénard, R.; De Winter, J.; Coulembier, O. Cyclic Polymers: Advances in Their Synthesis, Properties, and Biomedical Applications. *J. Polym. Sci.* **2020**, *58* (11), 1481−1502.
(38) Yol, A. M.; Dabney, D. E.; Wang, S.-F. F.; Laurent, B. A.; Foster, M. D.; Quirk, R. P.; Grayson, S. M.; Wesdemiotis, C. Differentiation of Linear and Cyclic Polymer Architectures by MALDI Tandem Mass Spectrometry (MALDI-MS2). *J. Am. Soc. Mass Spectrom.* **2013**, *24*, 74−82.
(39) Crotty, S.; Gerişlioğlu, S.; Endres, K. J.; Wesdemiotis, C.; Schubert, U. S.; Gerişlioğlu, S.; Endres, K. J.; Wesdemiotis, C.; Schubert, U. S. Polymer Architectures via Mass Spectrometry and Hyphenated Techniques: A Review. *Anal. Chim. Acta* **2016**, *932*, 1−21.
(40) Ropartz, D.; Li, P.; Fanuel, M.; Giuliani, A.; Rogniaux, H.; Jackson, G. P. Charge Transfer Dissociation of Complex Oligosaccharides: Comparison with Collision-Induced Dissociation and Extreme Ultraviolet Dissociative Photoionization. *J. Am. Soc. Mass Spectrom.* **2016**, *27* (10), 1614−1619.
(41) Sasiene, Z. J.; Ropartz, D.; Rogniaux, H.; Jackson, G. P. Charge Transfer Dissociation of a Branched Glycan with Alkali and Alkaline Earth Metal Adducts. *J. Mass Spectrom.* **2021**, *56* (7), 1−10.
(42) Mendis, P. M.; Sasiene, Z. J.; Ropartz, D.; Rogniaux, H.; Jackson, G. P. Ultra-High-Performance Liquid Chromatography Charge Transfer Dissociation Mass Spectrometry (UHPLC-CTD-MS) as a Tool for Analyzing the Structural Heterogeneity in Carrageenan Oligosaccharides. *Anal. Bioanal. Chem.* **2022**, *414*, 303.
(43) Mendis, P. M.; Sasiene, Z. J.; Ropartz, D.; Rogniaux, H.; Jackson, G. P. Structural Characterization of Isomeric Oligogalacturonan Mixtures Using Ultrahigh-Performance Liquid Chromatography-Charge Transfer Dissociation Mass Spectrometry. *Anal. Chem.* **2021**, *93*, 2838−2847.
(44) Pepi, L. E.; Sasiene, Z. J.; Mendis, P. M.; Jackson, G. P.; Amster, I. J. Structural Characterization of Sulfated Glycosaminoglycans Using Charge-Transfer Dissociation. *J. Am. Soc. Mass Spectrom.* **2020**, *31*, 2143−2153.
(45) Buck-Wiese, H.; Fanuel, M.; Liebeke, M.; Hoang, K. L. M.; Pardo-Vargas, A.; Seeberger, P. H.; Hehemann, J.-H.; Rogniaux, H.; Jackson, G. P.; Ropartz, D. Discrimination of β-1,4-and β-1,3-Linkages in Native Oligosaccharides via Charge Transfer Dissociation Mass Spectrometry. *J. Am. Soc. Mass Spectrom.* **2020**, *31* (6), 1249−1259.
(46) Ropartz, D.; Li, P.; Jackson, G. P.; Rogniaux, H. Negative Polarity Helium Charge Transfer Dissociation Tandem Mass Spectrometry: Radical-Initiated Fragmentation of Complex Polysulfated Anions. *Anal. Chem.* **2017**, *89* (7), 3824−3828.
(47) Sasiene, Z. J.; Mendis, P. M.; Ropartz, D.; Rogniaux, H.; Jackson, G. P. The Influence of Na/H Exchange on the Charge Transfer Dissociation (CTD) Spectra of Mannuronic Acid Oligomers. *Int. J. Mass Spectrom.* **2021**, *468*, 1−10.
(48) Li, P.; Kreft, I.; Jackson, G. P. Top-Down Charge Transfer Dissociation (CTD) of Gas-Phase Insulin: Evidence of a One-Step, Two-Electron Oxidation Mechanism. *J. Am. Soc. Mass Spectrom.* **2018**, *29* (2), 284−296.
(49) Li, P.; Jackson, G. P. Charge Transfer Dissociation (CTD) Mass Spectrometry of Peptide Cations: Study of Charge State Effects and Side-Chain Losses. *J. Am. Soc. Mass Spectrom.* **2017**, *28* (7), 1271−1281.
(50) Hoffmann, W. D.; Jackson, G. P. Charge Transfer Dissociation (CTD) Mass Spectrometry of Peptide Cations Using Kiloelectronvolt Helium Cations. *J. Am. Soc. Mass Spectrom.* **2014**, *25* (11), 1939−1943.
(51) Bari, S.; Hoekstra, R.; Schlathölter, T. Peptide Fragmentation by KeV Ion-Induced Dissociation. *Phys. Chem. Chem. Phys.* **2010**, *12* (14), 3376−3383.
(52) Sasiene, Z. J.; Mendis, P. M.; Jackson, G. P. Quantitative Assessment of Six Different Reagent Gases for Charge Transfer Dissociation (CTD) of Biological Ions. *Int. J. Mass Spectrom.* **2021**, *462*, 1−14.
(53) Butler, P. A.; Kräutler, B. Biological Organometallic Chemistry of B12. In *Bioorganometallic Chemistry*; Springer: Berlin, Heidelberg, 2006; Vol. *17*, pp 1−55. DOI: DOI: 10.1007/3418_004.
(54) Tran, J. C.; Doucette, A. A. Cyclic Polyamide Oligomers Extracted from Nylon 66 Membrane Filter Disks as a Source of Contamination in Liquid Chromatography/Mass Spectrometry. *J. Am. Soc. Mass Spectrom.* **2006**, *17* (5), 652−656.
(55) Schweighuber, A.; Gall, M.; Fischer, J.; Liu, Y.; Braun, H.; Buchberger, W. Development of an LC-MS Method for the Semiquantitative Determination of Polyamide 6 Contaminations in Polyolefin Recyclates. *Anal. Bioanal. Chem.* **2021**, *413*, 1091−1098.
(56) Li, P.; Hoffmann, W. D.; Jackson, G. P. Multistage Mass Spectrometry of Phospholipids Using Collision-Induced Dissociation (CID) and Metastable Atom-Activated Dissociation (MAD). *Int. J. Mass Spectrom.* **2016**, *403*, 1−7.
(57) Crowe, M. C.; Brodbelt, J. S.; Goolsby, B. J.; Hergenrother, P. Characterization of Erythromycin Analogs by Collisional Activated Dissociation and Infrared Multiphoton Dissociation in a Quadrupole Ion Trap. *J. Am. Soc. Mass Spectrom.* **2002**, *13*, 630−649.
(58) Lai, C. C.; Tsai, P. L.; Yu, C.; Her, G. R. Analysis of a Commercial Preparation of Erythromycin Estolates by Tandem Mass Spectrometry and High Performance Liquid Chromatography/Electrospray Ionization Tandem Mass Spectrometry Using an Ion Trap Mass Spectrometer. *Rapid Commun. Mass Spectrom.* **2000**, *14* (6), 468−475.
(59) Carraher, C. E. Synthesis of Caprolactam and Nylon 6. *J. Chem. Educ.* **1978**, *55* (1), 51−52.

(60) Palmer, R. Polyamides, Plastics. In *Encyclopedia of Polymer Science and Technology*; John Wiley & Sons, Inc., 2001. DOI: DOI: 10.1002/0471440264.pst251.
(61) Polce, M. J.; Ocampo, M.; Quirk, R. P.; Leigh, A. M.; Wesdemiotis, C. Tandem Mass Spectrometry Characteristics of Silver-Cationized Polystyrenes: Internal Energy, Size, and Chain End versus Backbone Substituent Effects. *Anal. Chem.* **2008**, *80*, 355−362.
(62) Cooper, H. J.; Håkansson, K.; Marshall, A. G. The Role of Electron Capture Dissociation in Biomolecular Analysis. *Mass Spectrom. Rev.* **2005**, *24* (2), 201−222.

https://doi.org/10.1021/jasms.1c00369
J. Am. Soc. Mass Spectrom. 2022, 33, 671−680